Icarus **149**, 235–250 (2001)
doi:10.1006/icar.2000.6533, available online at http://www.idealibrary.com on IDEAL®

High-Accuracy Statistical Simulation of Planetary Accretion: II. Comparison with *N*-Body Simulation

Satoshi Inaba

Department of Terrestrial Magnetism, Carnegie Institution of Washington, 5241 Broad Branch Road, Washington, DC 20015
E-mail: inaba@dtm.ciw.edu

Hidekazu Tanaka

Department of Earth and Planetary Sciences, Faculty of Science, Tokyo Institute of Technology, Tokyo 152-8551, Japan; and Southwest Research Institute, Boulder Colorado 80302

Kiyoshi Nakazawa

Department of Earth and Planetary Sciences, Faculty of Science, Tokyo Institute of Technology, Tokyo 152-8551, Japan

George W. Wetherill

Department of Terrestrial Magnetism, Carnegie Institution of Washington, 5241 Broad Branch Road, Washington, DC 20015

and

Eiichiro Kokubo

Department of Astronomy, Faculty of Science, University of Tokyo, Hongo, Bunkyo-Ku, Tokyo 113-0033, Japan

Received December 2, 1999; revised July 17, 2000

We have constructed an improved statistical method for the calculation of planetary accumulation using the currently standard model of terrestrial planet formation and using the latest results of planetary dynamical theory. The method is applicable for the range of masses in which velocity changes are dominated by gravitational forces, mutual collisions, and gas drag. Calculations are reported both with and without nebular gas. This method has been compared with *N*-body simulations, and the results of the two calculations are in agreement. As in earlier calculations, the growth of bodies in this mass range and at 1 AU occurs on a $\sim 10^5$ year time scale and is characterized by the evolution of an initially continuous mass distribution into a bimodal distribution, the high mass end of which consists of runaway bodies in the size range of $\sim 10^{26}$ g. In this general way, these results are in agreement with those reported earlier (e.g., Wetherill and Stewart 1993, *Icarus* 106, 190–209), but significant differences are also found as a result of the greater precision of the collision rate and the velocity evolution rate of planetesimals used in the present work.

Key Words: **planetary formation; planetesimals; computer techniques; planetary accretion; *N*-body simulation.**

1. INTRODUCTION

Planetesimal dynamical investigations have shown that the random velocity of a large body is suppressed through dynamical friction by small bodies and leads to the occurrence of runaway growth in planetary accumulation (e.g., Wetherill and Stewart 1989, Ida and Makino 1992b). This runaway growth is a mode of accumulation for which a few large bodies grow much faster than the other bodies. As a consequence, the growth of "Mars-size" bodies at 1 AU can occur ~100 times faster than when this effect is not included.

Planetary accumulation has been investigated by use of two techniques: *N*-body numerical integration and statistical transport theory. In *N*-body simulations (Kokubo and Ida 1996, 1998, 2000), the orbital evolution of all the bodies (planetesimals) are integrated numerically, calculating gravitational forces and collisions. Planetary growth occurs when two bodies collide and merge into one. In *N*-body simulations no approximation is included except perfectly inelastic collision. This method describes the accumulation process precisely. However, *N*-body simulations require long computing times and the number of

0019-1035/01 $35.00

available bodies is limited to $\sim 10^4$ at present. In the early stage of planetary growth, on the other hand, the number of planetesimals must be $>10^8$. Therefore, it is not feasible to investigate the accumulation process by N-body simulations alone.

To investigate the accumulation of a large number of planetesimals, one must make use of the statistical method (e.g., Greenberg *et al*. 1978; Nakagawa *et al*. 1983; Ohtsuki *et al*. 1988; Barge and Pellat 1991; Spaute *et al*. 1991; Wetherill and Stewart 1989, 1993; Weidenschilling *et al*. 1997; Kenyon and Luu 1998). The use of the statistical method makes it possible to study accumulation of planetesimals $\sim$1 km in diameter to form the largest planetary bodies $\sim$2000 km in diameter. In the statistical method, the time evolution of the distribution of the size and velocity of the planetesimals is calculated. This method has the merit of handling a large number of bodies because it does not treat physical quantities of individual bodies but only averaged quantities. As a result, the computing time of the accumulation process is much shorter than that of N-body simulations. At the same time, the statistical method has disadvantages. Physical quantities that characterize the mass distribution and the kinetic behavior of the planetesimals are all expressed only by averaged quantities. Because the planetary accumulation process involves strongly nonlinear phenomena, if the averaging is not done properly, the solution can be seriously disturbed and can fail to predict the process of planetary growth. Furthermore, after runaway growth of a few large bodies occurs, these cannot be completely described by the statistical manner alone (see Section 3.1). Thus, it is important to develop a statistical code that can provide precisely and efficiently those aspects of the accumulation process for which it is best suited. N-body simulations and the statistical method are complementary to each other. Both methods are necessary in the investigation of planetary accumulation.

In a series of papers, we are describing a new statistical numerical code for calculating the planetary accumulation process with high accuracy. Following the approach of Wetherill and Stewart (1989), we have already developed a statistical numerical code that accurately describes the accumulation process (Inaba *et al*. 1999, henceforth called Paper I). This statistical code contains some parameters that control the accuracy and the efficiency of the computation. Two parameters are essentially important: the parameter that determines the mass ratio of adjacent mass batches and the parameter that defines the length of time step of the accumulation algorithm. Through a number of numerical simulations for simple cases where the collision rate depended on only the masses of colliding bodies, we checked the validity of the statistical code by comparison with the analytical solutions to the stochastic coagulation equation (Marcus 1968, Tanaka and Nakazawa 1993) and found suitable values of these parameters (see Paper I).

In the present paper, we establish a statistical method that describes precisely the velocity evolution of planetesimals as well as their accumulation. In the planetary accumulation process, the mass-dependent eccentricities and inclinations of the planetesimals play an important role, because the collision rate is strongly dependent on these quantities. During the past decade, the collision rate and the velocity evolution of planetesimals have been investigated in detail (e.g., Ida and Nakazawa 1989, Greenzweig and Lissauer 1992, Ida 1990). In our code, we use the expression of the collision rates given by Greenzweig and Lissauer (1992) which included the Rayleigh-type distribution of the eccentricities and inclinations of planetesimals as well as the 3-body effects resulting from the central star's gravitational attraction. For the velocity evolution of planetesimals, we adopt the latest results of Stewart and Ida (2000; henceforth called SI00). The reliability of these results was verified by comparison with the results of N-body simulations. We also compare the results obtained by our new statistical code with those of N-body simulations in order to check the accuracy of our numerical code.

It is necessary to remember that our treatment is still simplified because real planet formation is quite complicated. Some important phenomena (e.g., collisional fragmentation of planetesimals and radial migration) are not included. In the future, we plan to include these and other phenomena, and to use the present work as a basis for our effort to draw the picture of planetary formation as realistically as possible.

In Section 2, we will describe the statistical coagulation equation as well as the other basic equations relevant to the basic processes of planetary accumulation, that is, (1) the collision rate between planetesimals, (2) the random velocity change resulting from mutual perturbation, and (3) the decreases in velocity caused by gas drag and inelastic collisions. The numerical method is described in Section 3. In Section 4, we will test the accuracy of our statistical method by comparing our numerical results with those of N-body simulation. We will see that our results agree well with those of N-body simulations. This section also considers the relationship between the present and previous works on this problem. The results are summarized and discussed in Section 5.

2. BASIC EQUATIONS FOR PLANETARY ACCUMULATION

2.1. Statistical Coagulation Equation

We consider a large number of bodies (planetesimals) rotating around a central star with mass M_c. We assume that the masses of the bodies are much smaller than M_c. We also assume that the eccentricity and the inclination of each body are much smaller than unity. In such a case, the bodies form a disk-like system around the central star. We denote the surface number density of planetesimals with masses between m and $m + dm$ by $n_s(m)\,dm$. Generally, $n_s(m)$ also depends on the distance from the central star. We assume that the accumulation process takes place in a toroidal region with a radius a and a narrow width Δa, and that $n_s(m)$ is uniform in this region. If quite large runaway bodies are formed and affect the spatial distribution of planetesimals, this assumption will not be valid.

Let us consider collisions between two populations of planetesimals that belong to mass ranges $(m_1, m_1 + dm_1)$ and $(m_2, m_2 + dm_2)$. The collision rate depends on the distributions of eccentricity and inclination in each population. As shown by Ida and Makino (1992a), the distribution function of the eccentricity, e_j, and the inclination, i_j, of planetesimals with mass m_j is well described by the Rayleigh-type distribution function $f_{\rm R}(e_j, i_j; e_j^*, i_j^*)$

$$f_{\rm R}(e_j, i_j; e_j^*, i_j^*)\, de_j\, di_j \equiv \frac{4 e_j i_j}{e_j^{*2} i_j^{*2}} \exp\left(-\frac{e_j^2}{e_j^{*2}} - \frac{i_j^2}{i_j^{*2}}\right) de_j\, di_j, \tag{1}$$

where e_j^* and i_j^* are the dispersions of e_j and i_j, respectively. The averaged number of collisions between two populations of planetesimals per unit area of the disk and per unit time, $\langle \Gamma_{\rm col} \rangle_{12}$, is given by Nakazawa *et al*. (1989) and Ohtsuki (1999) as

$$\langle \Gamma_{\rm col} \rangle_{12} = h_{12}^2 a^2 \Omega_{\rm K} n_{\rm s}(m_1) n_{\rm s}(m_2)\, dm_1\, dm_2 \langle P_{\rm col} \rangle_{12}, \tag{2}$$

where $\langle P_{\rm col} \rangle_{12}$ is the nondimensional mean collision rate between planetesimals with masses m_1 and m_2 (i.e., the collision rate, $P_{\rm col}$, averaged by the Rayleigh distribution function $f_{\rm R}(e, i; e^*, i^*)$ of each population), a is the semimajor axis, $\Omega_{\rm K}$ is the Keplerian angular velocity, and h_{12} is the reduced Hill radius of two planetesimals with masses m_1 and m_2 given by

$$h_{12} \equiv \left(\frac{m_1 + m_2}{3 M_{\rm c}}\right)^{1/3}. \tag{3}$$

Greenzweig and Lissauer (1992) made a detailed investigation of the collision rate between a protoplanet in a circular orbit and the ensemble of planetesimals with the Rayleigh-type distribution of eccentricities and inclinations, which is equivalent with that between planetesimals with the Rayleigh-type distribution as shown in Ohtsuki (1999). In the present study we use their results, as presented in the next section.

Using Eq. (2), we can express the coagulation equation for the disk system

$$\begin{aligned}\frac{dn_{\rm s}(m_1)}{dt} = {} & \frac{1}{2}\Omega_{\rm K} \int_0^{m_1} dm_2 \int_0^{\infty} dm_3 (h_{23} a)^2 n_{\rm s}(m_2) n_{\rm s}(m_3) \\ & \times \langle P_{\rm col} \rangle_{23} \delta(m_1 - m_2 - m_3) - \Omega_{\rm K} n_{\rm s}(m_1) \\ & \times \int_0^{\infty} dm_2 (h_{12} a)^2 n_{\rm s}(m_2) \langle P_{\rm col} \rangle_{12},\end{aligned} \tag{4}$$

where $\delta(x)$ is the delta function and has the characteristic

$$\int_{-\infty}^{\infty} dx f(x) \delta(x - a) = f(a). \tag{5}$$

Equation (4) is the basic equation describing the evolution of the mass distribution function $n_{\rm s}(m)$. The first term on the right-hand side represents the formation of the bodies with mass m_1 by the coalescence of bodies with masses m_2 and m_3. The factor of $1/2$ is introduced to prevent double counting. The second term describes the loss of the bodies with mass m_1 by coalescence with other bodies and the formation of larger bodies.

2.2. Collision Rate between Planetesimals

Prior to the description of the mean collision rate, we introduce the reduced relative eccentricity, $\tilde{e}$, and the reduced relative inclination, $\tilde{i}$, which are defined as (Nakazawa *et al*. 1989)

$$\tilde{e} \equiv e/h_{12} \quad \text{and} \quad \tilde{i} \equiv i/h_{12}, \tag{6}$$

respectively. The reduced relative dispersions $\tilde{e}^*$ and $\tilde{i}^*$ are also defined in the same way. The mean collision rate depends on $\tilde{e}^*$ and $\tilde{i}^*$. For the sake of simplicity we frequently eliminate the term "reduced" from the designation of $\tilde{e}$ or $\tilde{i}$ as long as there is no possibility of confusion. The case with $\tilde{e}, \tilde{i} \gtrsim 2$ is called the high-velocity regime, while the case with $\tilde{e}, \tilde{i} \lesssim 0.2$ is called the low-velocity regime.

The collision rate between planetesimals has been studied analytically or numerically by many researchers (e.g., Wetherill and Cox 1985; Ida and Nakazawa 1989; Greenzweig and Lissauer 1990, 1992; Dones and Tremaine 1993). Greenzweig and Lissauer (1990, 1992) gave an analytic formula of the mean collision rate for the high-velocity regime ($\tilde{e}, \tilde{i} \gtrsim 2$): the collision rate $P_{\rm col}$ is approximately given by

$$P_{\rm col}(\tilde{e}, \tilde{i})_{\rm high} = \frac{\tilde{r}_{\rm p}^2}{2\pi}\left(F(I) + \frac{6}{\tilde{r}_{\rm p}} \frac{G(I)}{\tilde{e}^2}\right), \tag{7}$$

where

$$\tilde{r}_{\rm p} \equiv \frac{r_1 + r_2}{h_{12} a}, \tag{8}$$

and r_1 and r_2 are the radii of colliding planetesimals and $I \equiv \tilde{i}/\tilde{e}$. Functions $F(I)$ and $G(I)$ are defined, respectively, by

$$F(I) \equiv \frac{4\sqrt{1 + I^2}}{I} E(k) \quad \text{and} \quad G(I) \equiv \frac{4}{I\sqrt{1 + I^2}} K(k), \tag{9}$$

where $K(k)$ and $E(k)$ are the complete elliptic integrals of the first and the second kinds, respectively, and $k^2 \equiv 3/(4 + 4I^2)$. Averaging over the distribution function, the mean collision rate $\langle P_{\rm col} \rangle$ is

$$\langle P_{\rm col} \rangle_{\rm high} = \frac{\tilde{r}_{\rm p}^2}{2\pi}\left(\mathcal{F}(I^*) + \frac{6}{\tilde{r}_{\rm p}} \frac{\mathcal{G}(I^*)}{\tilde{e}^{*2}}\right), \tag{10}$$

where $I^* \equiv \tilde{i}^*/\tilde{e}^*$ and the functions $\mathcal{F}(I^*)$ and $\mathcal{G}(I^*)$ are given,

respectively, by

$$\mathcal{F}(I^*) \equiv 8\int_0^1 d\lambda \frac{I^{*2}E[\sqrt{3(1-\lambda^2)}/2]}{[I^{*2}+(1-I^{*2})\lambda^2]^2} \tag{11}$$

and

$$\mathcal{G}(I^*) \equiv 8\int_0^1 d\lambda \frac{K[\sqrt{3(1-\lambda^2)}/2]}{[I^{*2}+(1-I^{*2})\lambda^2]}. \tag{12}$$

In Eq. (10), the second term expresses the enhancement of the collision rate due to gravitational focusing. When this term becomes larger than the first term, runaway growth occurs (Wetherill 1990, Ohtsuki *et al*. 1993).

For the low-velocity regime ($\tilde{e}, \tilde{i} \lesssim 0.2$), Ida and Nakazawa (1989) found that the collision rate $P_{\rm col}$ becomes insensitive to $\tilde{e}$ and $\tilde{i}$ and approaches

$$\langle P_{\rm col}\rangle_{\rm low} = 11.3\sqrt{\tilde{r}_{\rm p}} \tag{13}$$

as $(\tilde{e}, \tilde{i})$ approach zero. Furthermore, for the medium regime ($0.2 \lesssim \tilde{e}, \tilde{i} \lesssim 2$), it was shown that the collision rate depends on only $\tilde{i}$ in Ida and Nakazawa (1989) and is given by

$$\langle P_{\rm col}\rangle_{\rm med} = \frac{\tilde{r}_{\rm p}^2}{4\pi\tilde{i}^*}\left(17.3+\frac{232}{\tilde{r}_{\rm p}}\right). \tag{14}$$

In a system of planetesimals, it is known that $\tilde{i}^*$ is on the same order of magnitude as $\tilde{e}^*$. We find that the mean collision rate is well approximated by the following simple expression over the entire range of $(\tilde{e}^*, \tilde{i}^*)$:

$$\langle P_{\rm col}\rangle = \min\left(\langle P_{\rm col}\rangle_{\rm med}, \left(\langle P_{\rm col}\rangle_{\rm high}^{-2} + \langle P_{\rm col}\rangle_{\rm low}^{-2}\right)^{-1/2}\right). \tag{15}$$

In Fig. 1, mean collision rates evaluated by using the above expression are compared with the results of the 3-body numerical calculations of Greenzweig and Lissauer (1992), for the cases of $\tilde{e}^* = \tilde{i}^*$, $2\tilde{i}^*$, and $4\tilde{i}^*$. The approximate formula (15) reproduces the numerical results within an error of a factor of 2. In the present study, we use this expression for the mean collision rate between planetesimals.

2.3. Velocity Evolution of Planetesimals

Because the mean collision rates between the planetesimals depend on the dispersions of their eccentricities and inclinations, those dispersions must be calculated precisely. The dispersions depend in turn on the mass of the planetesimals, and hence, it is necessary to evaluate the dispersions $\tilde{e}_j^*$ and $\tilde{i}_j^*$ for each mass m_j. During each time interval, their dispersions change as a result of gravitational perturbations by other planetesimals and decrease by the drag due to the nebular gas, as well as by collisions. The time variation of the square of dispersions is given, as the sum

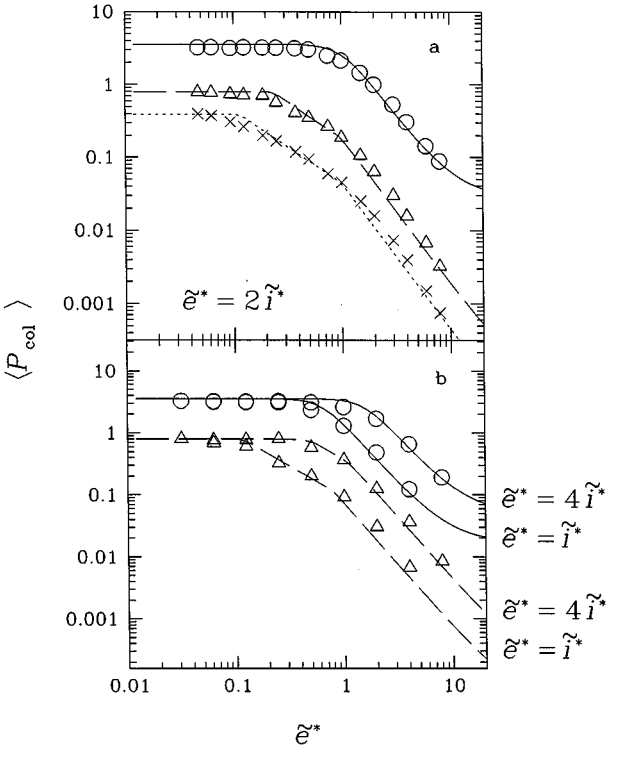

FIG. 1. Comparison of the mean collision rate $\langle P_{\rm col}\rangle$ evaluated from the approximate formula (curves) with those of the corresponding numerical solutions (circles, triangles, and crosses). The mean collision rate is shown as a function of $\tilde{e}^*$ for the cases of $\tilde{e}^* = 2\tilde{i}^*$ (a) and $\tilde{e}^* = \tilde{i}^*$ and $4\tilde{i}^*$ (b). In these panels solid, dashed, and dotted curves indicate the mean collision rate for $\tilde{r}_p = 0.1, 0.005$, and 0.0012, respectively.

of these three effects, by

$$\begin{cases} \dfrac{de_j^{*2}}{dt} = \left(\dfrac{de_j^{*2}}{dt}\right)_{\rm grav} + \left(\dfrac{de_j^{*2}}{dt}\right)_{\rm gas} + \left(\dfrac{de_j^{*2}}{dt}\right)_{\rm col}, \\ \dfrac{di_j^{*2}}{dt} = \left(\dfrac{di_j^{*2}}{dt}\right)_{\rm grav} + \left(\dfrac{di_j^{*2}}{dt}\right)_{\rm gas} + \left(\dfrac{di_j^{*2}}{dt}\right)_{\rm col}, \end{cases} \tag{16}$$

where terms with subscripts "grav," "gas," and "col" express the time variations due to the gravitational perturbation, the gas drag, and the collisions, respectively. Henceforth, we call simply e^* or i^* as "the random velocity." This is permissible because $(e^{*2}+i^{*2})^{1/2}v_{\rm K}$ is almost equal to the mean deviation of the velocity from the Keplerian circular velocity.

(a) Velocity evolution due to gravitational perturbation. Ida (1990), Ohtsuki (1999), and SI00 investigated the evolution of the dispersions of eccentricity and inclination due to mutual gravitational interaction. The time evolutions of e_1^{*2} and i_1^{*2} of planetesimals with mass m_1 were described, respectively, as

$$\left(\frac{de_1^{*2}}{dt}\right)_{\rm grav} = \Omega_{\rm K}a^2\int dm_2 n_{\rm s}(m_2)\frac{h_{12}^4 m_2}{(m_1+m_2)^2} \times\left(m_2\langle P_{\rm VS}\rangle + 0.7\langle P_{\rm DF}\rangle\frac{m_2e_2^{*2}-m_1e_1^{*2}}{i_{12}^{*2}}\right) \tag{17}$$

and

$$\left(\frac{di_1^{*2}}{dt}\right)_{\rm grav} = \Omega_{\rm K} a^2 \int dm_2 n_{\rm s}(m_2) \frac{h_{12}^4 m_2}{(m_1+m_2)^2} \times \left(m_2 \langle Q_{\rm VS}\rangle + 0.7 \langle Q_{\rm DF}\rangle \frac{m_2 i_2^{*2} - m_1 i_1^{*2}}{i_{12}^{*2}} \right). \quad (18)$$

The first terms in the brackets represent the change rate by viscous stirring due to encounters with other planetesimals and the second terms correspond to the change rate by dynamical friction, which leads to energy equipartition among planetesimals with different masses. As definitions of $\langle P_{\rm VS}\rangle$, $\langle P_{\rm DF}\rangle$, $\langle Q_{\rm VS}\rangle$, and $\langle Q_{\rm DF}\rangle$ we adopted those of Ohtsuki (1999), which are smaller than those of SI00 by a factor of h_{12}^4. SI00 derived analytic expressions for the mean viscous stirring rates, $\langle P_{\rm VS}\rangle$ and $\langle Q_{\rm VS}\rangle$, and the mean dynamical friction rates, $\langle P_{\rm DF}\rangle$ and $\langle Q_{\rm DF}\rangle$. In the present study, we use these analytical expressions with the exception of the factor of h_{12}^4 mentioned above.

(b) Velocity evolution due to gas drag. Adachi *et al.* (1976) investigated extensively the gas drag effect on the motion of a planetesimal rotating around the protosun. They obtained the approximate formulas of the time evolution of the semimajor axis, a, the eccentricity, e, and the inclination, i, averaging over one Keplerian period. Assuming that one of e, i, and η is much larger than others and retaining the leading terms, they obtain the approximate equations:

$$\frac{\tau}{a}\left(\frac{da}{dt}\right)_{\rm gas} = -2\eta\left(\frac{2(2E+K)}{3\pi}e + \frac{2}{\pi}i + \eta\right), \quad (19)$$

$$\frac{\tau}{e}\left(\frac{de}{dt}\right)_{\rm gas} = -\left(\frac{2E}{\pi}e + \frac{2}{\pi}i + \frac{3}{2}\eta\right), \quad (20)$$

and

$$\frac{\tau}{i}\left(\frac{di}{dt}\right)_{\rm gas} = -\frac{1}{2}\left(\frac{2E}{\pi}e + \frac{8}{3\pi}i + \eta\right), \quad (21)$$

where E and K are the elliptic integrals $E(3/4)$ and $K(3/4)$. In the above, η is a parameter describing the deviation of the gas velocity $v_{\rm gas}$ from Keplerian velocity $v_{\rm K}$ due to the radial pressure gradient in the gaseous disk and is defined by

$$\eta \equiv \frac{v_{\rm K} - v_{\rm gas}}{v_{\rm K}}. \quad (22)$$

The characteristic time for the drag dissipation, τ, is given by

$$\tau \equiv \left(\frac{1}{2} C_{\rm D} \pi r^2 \rho_{\rm gas} a \Omega_{\rm K}/m\right)^{-1}, \quad (23)$$

where $C_{\rm D}$ is the drag coefficient, r and m are the radius and mass of a planetesimal, respectively, and $\rho_{\rm gas}$ is the gas density of the solar nebula. As indicated by Kary *et al.* (1993), there is an error in the expression of de/dt of Adachi *et al.* (1976) (Eq. (4.12)). The coefficient of η should be $3/2$, not $1/2$.

As may be conjectured from the way Eqs. (20) and (21) were derived, errors of these equations become large when e, i, and η are comparable with one another. To avoid this fault, we propose the new equations

$$\frac{\tau}{a}\left(\frac{da}{dt}\right)_{\rm gas} = -2\eta\left[\left(\frac{2(2E+K)}{3\pi}e\right)^2 + \left(\frac{2}{\pi}i\right)^2 + \eta^2\right]^{1/2}, \quad (24)$$

$$\frac{\tau}{e}\left(\frac{de}{dt}\right)_{\rm gas} = -\left[\left(\frac{2E}{\pi}e\right)^2 + \left(\frac{2}{\pi}i\right)^2 + \left(\frac{3}{2}\eta\right)^2\right]^{1/2}, \quad (25)$$

and

$$\frac{\tau}{i}\left(\frac{di}{dt}\right)_{\rm gas} = -\frac{1}{2}\left[\left(\frac{2E}{\pi}e\right)^2 + \left(\frac{8}{3\pi}i\right)^2 + \eta^2\right]^{1/2}. \quad (26)$$

Although we cannot show the validity of the new equations analytically, we can confirm it numerically. In Fig. 2, we compare the time evolution of a, e, and i calculated from the equations of Adachi *et al.* (1976) and our new equations with the results

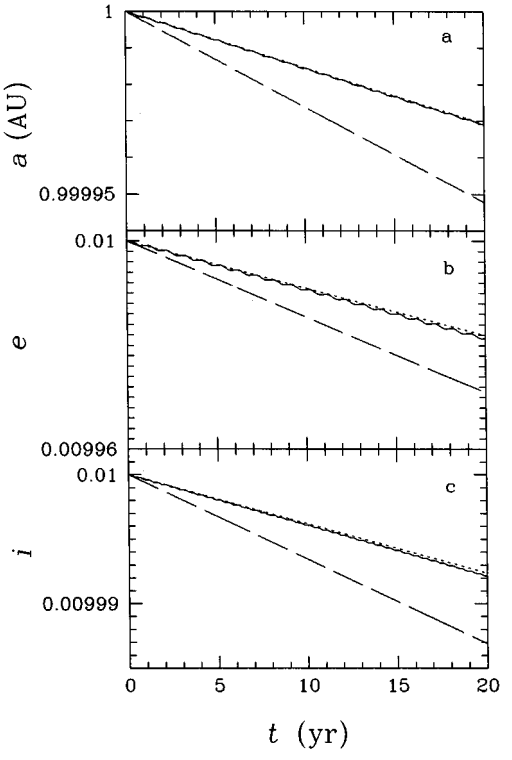

FIG. 2. Time evolution of the semimajor axis, a, the eccentricity, e, and the inclination, i, due to gaseous drag. These are calculated from the equations derived by Adachi *et al.* (1976) (dashed curves) and the new equations (dotted curves) as well as the orbital calculation (solid curves). For the initial condition we choose $e = i = 0.01$ and $a = 1$ AU and for τ and η we put to be $\tau = 200 T_{\rm K}$ and $\eta = 0.01$.

of the orbital calculation. (The comparison is made in the case where $\tau = 200T_K$ and $\eta = 0.01$. The initial conditions are $e = i = 0.01$ and $a = 1$ AU.) As seen in this figure, the new equations reproduce the results of the orbital calculation much better than those of Adachi *et al*.

Averaging each term separately by the distribution function of e and i (i.e., the Rayleigh-type distribution function) and summing them up in a similar way to Eqs. (24) to (26), we obtain the following equations for the dispersion e^* and i^* (note that the dispersions are not of the "reduced" type):

$$\frac{\tau}{e^{*2}}\left(\frac{de^{*2}}{dt}\right)_{\rm gas} = -2\left(\frac{9}{4\pi}E^2e^{*2} + \frac{1}{\pi}i^{*2} + \frac{9}{4}\eta^2\right)^{1/2} \quad (27)$$

and

$$\frac{\tau}{i^{*2}}\left(\frac{di^{*2}}{dt}\right)_{\rm gas} = -\left(\frac{1}{\pi}E^2e^{*2} + \frac{4}{\pi}i^{*2} + \eta^2\right)^{1/2}. \quad (28)$$

(c) Velocity evolution due to collision. Collisional dissipation is also important for the velocity evolution of planetesimals. Stewart and Wetherill (1988) derived the velocity evolution rate due to collisional dissipation, which was used by Wetherill and Stewart (1989, 1993). However, in the derivation, they assumed that collisions between the bodies occurred with zero rebound instead of complete accretion into a sphere, as we consider in the present paper. Ohtsuki (1992) examined velocity evolution due to collisional dissipation, assuming complete accretion. In the present paper, we adopt his method. It will be seen that the derived evolution rate is qualitatively different from that of Stewart and Wetherill (1988). When two planetesimals (with masses m_2 and m_3) coalesce, the orbit of a merged planetesimal is given by that of the center of mass. The eccentricity E_{23} and inclination I_{23} of the barycenter's orbit are given by (Ida 1990)

$$\begin{cases} E_{23}^2 = \left(\frac{m_2}{m_2+m_3}\right)^2 e_2^2 + \left(\frac{m_3}{m_2+m_3}\right)^2 e_3^2 + \frac{2m_2m_3}{(m_2+m_3)^2}e_2e_3\cos(\tau_2-\tau_3), \\ I_{23}^2 = \left(\frac{m_2}{m_2+m_3}\right)^2 i_2^2 + \left(\frac{m_3}{m_2+m_3}\right)^2 i_3^2 + \frac{2m_2m_3}{(m_2+m_3)^2}i_2i_3\cos(\omega_2-\omega_3), \end{cases} \quad (29)$$

where τ_j and ω_j are the longitude of the perihelion and the ascending node, respectively. Assuming the random distribution of the phase angles τ_j and ω_j and averaging by the Rayleigh-type distribution (1), we obtain the dispersions of E_{23} and I_{23} as (Ohtsuki 1992)

$$\begin{cases} E_{23}^{*2} = \left(\frac{m_2}{m_2+m_3}\right)^2 e_2^{*2} + \left(\frac{m_3}{m_2+m_3}\right)^2 e_3^{*2}, \\ I_{23}^{*2} = \left(\frac{m_2}{m_2+m_3}\right)^2 i_2^{*2} + \left(\frac{m_3}{m_2+m_3}\right)^2 i_3^{*2}. \end{cases} \quad (30)$$

Noting that coalescing bodies have the square of dispersions given by Eq. (30) and using the averaged number of collisions between two populations of planetesimals per unit area and per unit time given by Eq. (2), we obtain the variation rate of e_1^{*2} and i_1^{*2} of planetesimals with mass m_1 due to coalescence as

$$\left(\frac{de_1^{*2}}{dt}\right)_{\rm col} = -\frac{\Omega_K}{2n_s(m_1)}\int dm_2 \int dm_3 (h_{23}a)^2 n_s(m_2)n_s(m_3) \times \left(e_1^{*2} - E_{23}^{*2}\right)\langle P_{\rm col}\rangle_{23}\delta(m_1 - m_2 - m_3) \quad (31)$$

and

$$\left(\frac{di_1^{*2}}{dt}\right)_{\rm col} = -\frac{\Omega_K}{2n_s(m_1)}\int dm_2 \int dm_3 (h_{23}a)^2 n_s(m_2)n_s(m_3) \times \left(i_1^{*2} - I_{23}^{*\,2}\right)\langle P_{\rm col}\rangle_{23}\delta(m_1 - m_2 - m_3). \quad (32)$$

From the above expressions of the evolution rates, it can be shown that the evolution rates vanish when energy equipartition is satisfied in the velocity distribution (i.e., $e^*, i^* \propto m^{-1/2}$). Furthermore, when the velocity distribution has a steeper dependence on the mass, collisional dissipation increases the velocity dispersion e^* and i^*. This is because decrease in the number of planetesimals due to accretion makes the random energy per planetesimal increase despite collisional dissipation in the total random energy. As a result, collisional dissipation has an effect that makes the velocity distribution correspond to energy equipartition state, in addition to the equipartition resulting from the dynamical friction (Ohtsuki 1992). The velocity evolution rate derived by Stewart and Wetherill (1988) does not vanish in the case of energy equipartition and is also negative for a steeper velocity distribution. A more detailed comparison of collisional dissipation with the results of Stewart and Wetherill (1988) will be given in Section 4.2.

3. METHODS OF SIMULATION

The statistical simulation code for describing the accumulation process, especially, describing the runaway growth of planets, was developed by Wetherill and Stewart (1989) and discussed further in Wetherill (1990). As mentioned in the Introduction, Inaba *et al*. (1999) reconstructed the statistical simulation code based on Wetherill and Stewart and clarified the validity and usefulness of the code. Here, we describe briefly the numerical procedures of our code.

3.1. Evolution of the Mass Distribution

To describe the mass distribution of planetesimals, we use a set of discrete mass batches instead of the (continuous) mass coordinate used in the preceding equations. The initial mass m_j of the jth batch is given by a geometric series

$$m_j = m_0\Delta^j, \quad j = 0, 1, \ldots, n_b - 1 \quad (33)$$

where n_b is the total number of batches. The mass division parameter, Δ, is set equal to 1.1 in the present study. Inaba *et al*.

(1999) showed that simulation with $\Delta \leq 1.3$ can describe runaway growth precisely. Let $N_{s,j}$ be the surface number density of planetesimals belonging to batch j (i.e., with the mass m_j). A set of the surface number densities $\{N_{s,j}\}$ describes the mass distribution function $n_s(m)$. From Eq. (4), we can write the equation describing the time evolution of the surface number density $N_{s,l}$ as

$$\frac{dN_{s,l}}{dt} = \frac{1}{2}\Omega_K \sum_{j,k;l}{}' (h_{jk}a)^2 N_{s,j} N_{s,k} \langle P_{col}\rangle_{jk} - \Omega_K N_{s,l} \sum_j (h_{jl}a)^2 N_{s,j} \langle P_{col}\rangle_{jl}, \quad (34)$$

where $\sum'_{j,k;l}$ is the sum over the pair of batches j and k which satisfy $(m_l + m_{l-1})/2 < m_j + m_k < (m_l + m_{l+1})/2$. In the simulation, instead of the surface number density $N_{s,j}$, we calculate the number of planetesimals in the toroidal region, which is given by

$$N_j = 2\pi a \Delta a N_{s,j}, \quad (35)$$

where a and Δa are the radius and the width of the toroidal region, respectively.

Equation (34) is integrated following the flow chart shown in Fig. 3. During a (numerical) time interval δt the number of collisions between bodies belonging to a target batch (j) and a projectile batch ($k; k \leq j$), $\delta N_{col,jk}$, is given by

$$\delta N_{col,jk} = h_{jk}^2 a^2 \Omega_K N_{s,j} N_k \langle P_{col}\rangle_{jk} \delta t. \quad (36)$$

The growth of bodies belonging to batch j in a time interval δt is treated in two ways. If the mass of merged bodies, $m_j + m_k$, is smaller than $(m_j + m_{j+1})/2$, then the bodies still belong to batch j; the number of bodies in batch k is decreased by $\delta N_{col,jk}$ and the number of bodies in batch j remains unchanged, whereas the total mass in batch j is increased by $m_k \delta N_{col,jk}$ and the total mass in batch k is decreased by $m_k \delta N_{col,jk}$ (structures (7) and (8) in Fig. 3). On the other hand, if the combined mass, $m_j + m_k$, is greater than $(m_j + m_{j+1})/2$, then the merged bodies are placed into a higher batch (say, batch l); the numbers of bodies in both batches j and k are decreased by $N_{col,jk}$ and the total masses in batches j and k are decreased by $m_j \delta N_{col,jk}$ and $m_k \delta N_{col,jk}$, respectively. Furthermore, the number of bodies in batch l is increased by $\delta N_{col,jk}$ and its mass is increased by $(m_j + m_k)\delta N_{col,jk}$ (structures (7) and (9) in Fig. 3). We repeat the above procedures for all pairs of batches j and k.

Defining N_j^n as the number of bodies in batch j at time $t = t_n$, we can calculate the net changes in the number δN_j and the mass δM_j for each batch. The number of bodies of batch j at time $t_{n+1} = t_n + \delta t$ is then given by

$$N_j^{n+1} = N_j^n + \delta N_j. \quad (37)$$

Furthermore, a new average mass of batch j is evaluated by dividing the newly obtained total mass by the newly obtained number of bodies contained in the batch. That is,

$$m_j^{n+1} = \left(M_j^n + \delta M_j\right) / N_j^{n+1} \quad (38)$$

(structures (10) and (11) in Fig. 3).

In order to keep the number of planetesimals N_j an integer, we make $\delta N_{col,jk}$ an integer. If $\delta N_{col,jk} < 2 \times 10^9$ (the maximum integer expressed by 32-bit computer memory, i.e., 2^{31}), $\delta N_{col,jk}$ is replaced by (Wetherill and Stewart 1993, Paper I)

$$\delta N'_{col,jk} = [\delta N_{col,jk}] + \epsilon, \quad (39)$$

where $[\delta N_{col,jk}]$ is the integer part of $\delta N_{col,jk}$ and ϵ is given by

$$\epsilon = \begin{cases} 1 & : \delta N_{col,jk} - [\delta N_{col,jk}] \geq \zeta \\ 0 & : \delta N_{col,jk} - [\delta N_{col,jk}] < \zeta, \end{cases} \quad (40)$$

with ζ a random number between 0 and 1. On the other hand, if $\delta N_{col,jk}$ is equal to or greater than 2×10^9, we permit $\delta N_{col,jk}$ to be a fractional value (structures (5) and (6) in Fig. 3).

Furthermore, another device is introduced to describe runaway bodies properly. Kokubo and Ida (1998) and Weidenschilling *et al.* (1997) showed that when runaway bodies are formed in a swarm of planetesimals, the radial separation of their orbits tends to be about 10 times as large as the mutual Hill radius of the bodies (Eq. (3)). This phenomenon is termed "oligarchic growth." The orbits of the runaway bodies are nearly circular and coplanar because of dynamical friction from the small bodies. Orbits of these runaway bodies never cross on the time scale of our calculation and therefore they cannot collide with each other. Following Wetherill and Stewart (1993), we take account of this isolation of the bodies in the following way. Let $N_{runaway}$ be the total number of these largest isolated runaway bodies, defined such that the sum of their orbital separations δa_i is equal to the width of the computation zone, Δa. In the simulation, the bodies contained in all batches more massive than batch j' are assumed to be isolated, where the batch number j' is defined by the condition

$$\sum_{i=j'+1}^{n_b-1} N_i \delta a_i < \Delta a < \sum_{i=j'}^{n_b-1} N_i \delta a_i. \quad (41)$$

By the use of j', $N_{runaway}$ is given by

$$N_{runaway} \equiv \sum_{i=j'}^{n_b-1} N_i. \quad (42)$$

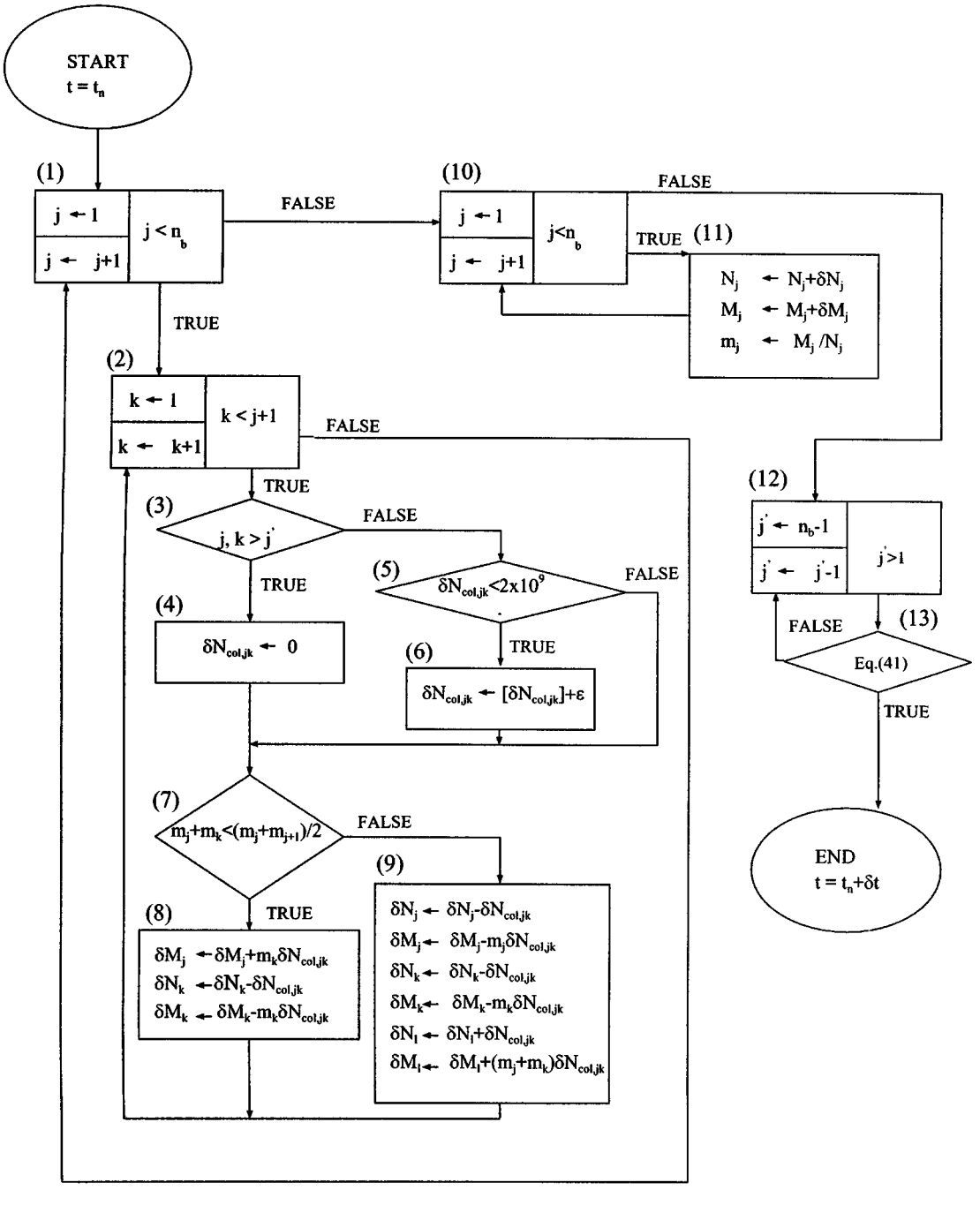

FIG. 3. Flow chart displaying the process described in Section 3.1. The procedure is shown for a single time step from $t = t_n$ to $t_n + \delta t$. The flow chart has three distinct structures—squares with partitions, squares without partitions, and diamonds. In the partitioned squares, initial and subsequent commands are on the upper and lower left sides, respectively. In the initial command the counter is initialized (e.g., $j = 1$). If the statement in the right section is correct, flow proceeds following the TRUE arrow. Otherwise, flow proceeds following the FALSE arrow. If flow returns to a partitioned square, the subsequent commands in the lower left are carried out, where the counter is incremented. In a square without partition, values of variables are updated. A command in a diamond follows the same rules as the statements in the right side of squares with partitions. In the diagram, $\delta N_{\mathrm{col},jk}$ is the number of collisions during a (numerical) time interval δt between bodies belonging to a target batch (j) and a projectile batch ($k; k \leq j$), δN_j and δM_j are the net changes in the number and the mass for each batch, and ϵ is given by Eq. (40).

Furthermore, the orbital separation, δa_i, is defined by

$$\delta a_i \equiv 10\left(\frac{m_i + m_{\rm runaway}}{3M_c}\right)^{1/3} a, \tag{43}$$

where the numerical factor 10 comes from the results of Kokubo and Ida (1998) and $m_{\rm runaway}$ is the mean mass of the runaway bodies:

$$m_{\rm runaway} \equiv \sum_{i=j'}^{n_{\rm b}-1} m_i N_i \Big/ N_{\rm runaway} \tag{44}$$

(structures (12) and (13) in Fig. 3).

In the runaway growth stage as well as the oligarchic growth stage, masses of the runaway bodies do not differ much and it is adequate to adopt the mean mass of runaway bodies in Eq. (42). The choice of the separation δa_i will be justified in Section 4.

3.2. Evolution of Eccentricity and Inclination

From Eqs. (17) and (18), we can write the equations describing the time evolution of e_l^{*2} and i_l^{*2} of planetesimals belonging to batch l due to the gravitational interaction

$$\left(\frac{de_l^{*2}}{dt}\right)_{\rm grav} = \Omega_{\rm K} a^2 \sum_{j=0}^{n_{\rm b}-1} \left(\frac{N_j - \delta_{jl}}{2\pi a \Delta a}\right) \frac{h_{jl}^4 m_j}{(m_j + m_l)^2} \times \left(m_j \langle P_{\rm VS}\rangle + 0.7\langle P_{\rm DF}\rangle \frac{m_j e_j^{*2} - m_l e_l^{*2}}{e_{jl}^{*\,2}}\right) \tag{45}$$

and

$$\left(\frac{di_l^{*2}}{dt}\right)_{\rm grav} = \Omega_{\rm K} a^2 \sum_{j=0}^{n_{\rm b}-1} \left(\frac{N_j - \delta_{jl}}{2\pi a \Delta a}\right) \frac{h_{jl}^4 m_j}{(m_j + m_l)^2} \times \left(m_j \langle Q_{\rm VS}\rangle + 0.7\langle Q_{\rm DF}\rangle \frac{m_j i_j^{*2} - m_l i_l^{*2}}{i_{jl}^{*\,2}}\right), \tag{46}$$

where δ_{jl} is the Kronecker delta. Except for the gravitational interactions between the runaway bodies, we use the same expressions for $\langle P_{\rm VS}\rangle$, $\langle Q_{\rm VS}\rangle$, $\langle P_{\rm DF}\rangle$, and $\langle Q_{\rm DF}\rangle$ as SI00. We must pay special attention to the gravitational interaction between the runaway bodies since their orbits do not cross. For the stirring rate and the dynamical friction rate of the runaway bodies, we use the distant encounter expression of

$$\langle P_{\rm VS}\rangle = 1.6, \tag{47}$$

and

$$\langle P_{\rm DF}\rangle = \langle Q_{\rm VS}\rangle = \langle Q_{\rm DF}\rangle = 0. \tag{48}$$

The detailed derivation of $\langle P_{\rm VS}\rangle$ is given in the Appendix.

As described in Section 2, e^* and i^* decrease as a result of gas drag as well as collisional dissipation. The changes in eccentricity and inclination due to gas drag are calculated according to Eqs. (27) and (28). The evolution of e_l^* and i_l^* due to collision is described by Eqs. (31) and (32). In our numerical simulation, the new values of e_l^{*2} and i_l^{*2} of batch l are given, respectively, by

$$e_{l,\rm new}^{*2} = e_l^{*2} - \frac{\sum'_{j,k;l} \left(e_l^{*2} - E_{jk}^{*2}\right)\delta N_{{\rm col},jk}}{N_l} \tag{49}$$

and

$$i_{l,\rm new}^{*2} = i_l^{*2} - \frac{\sum'_{j,k;l} \left(i_l^{*2} - I_{jk}^{*\,2}\right)\delta N_{{\rm col},jk}}{N_l} \tag{50}$$

where the sum $\sum'_{j,k;l}$ has the same meaning as that in Eq. (34). The second terms on the right-hand side of the above equations represent the variations of dispersions of eccentricity and inclination by the coalescence during a time interval and are obtained from Eqs. (31) and (32).

4. COMPARISONS

4.1. Comparisons with N-Body Simulation

Kokubo and Ida (1998, 2000) performed N-body simulations of planetary accumulation in a toroidal region around $a = 1$ AU. They considered two cases (i.e., cases with and without nebular gas). In order to compare our calculations with their N-body simulations, we have performed the numerical simulation using the same parameters. The values of the parameters are shown in Table I. In the N-body simulation without nebular gas, the radius of a planetesimal was magnified artificially by a factor of 6 to save computational time.

As pointed out by Inaba *et al.* (1999), in a single run of the simulation the mass distribution evolves discontinuously owing to the stochastic behavior of coalescence. In order to remove this fluctuation, we take an ensemble mean for a large number

TABLE I
Adopted Parameters for the Simulation

Quantity	Symbol	Value
Distance from the protosun (AU)	a	1
Ring width (AU)	Δa	0.092 (with nebular gas) 0.021 (without nebular gas)
Material density of planetesimals (g/cm^3)	$\rho_{\rm mat}$	2 (with nebular gas) $2/6^3$ (without nebular gas)
Gas drag coefficient	$C_{\rm D}$	2
Nebular gas density (g/cm^3)	$\rho_{\rm gas}$	2×10^{-9} (with nebular gas) 0 (without nebular gas)
	η	1.85×10^{-3}

Note. η is a nondimensional parameter defined by Eq. (22).

of independent runs. The ensemble mean of a quantity X at time t, X, is given by

$$X \equiv \frac{1}{n_{\rm run}} \sum_{m=1}^{n_{\rm run}} X^m, \tag{51}$$

where $n_{\rm run}$ is the number of the independent simulations (in our present study, we adopt $n_{\rm run} = 100$) and X^m is the quantity at time t, obtained by the mth run.

Furthermore, in order to evaluate magnitude of the fluctuation, we calculate a standard deviation, σ_X, defined as

$$\sigma_X \equiv \sqrt{\frac{\sum_{m=1}^{n_{\rm run}} (X^m - X)^2}{n_{\rm run}}}. \tag{52}$$

We consider four physical quantities X^m: the cumulative numbers of the mass distribution, the root mean squares of the eccentricity and the inclination of a swarm of planetesimals, the root mean square of masses of planetesimals, and the mass of the largest planetesimal. The cumulative number $N_{\rm c}(m_j)$ is defined as the sum of the number of planetesimals with mass larger than m_j

$$N_{\rm c}(m_j) \equiv \sum_{k=j}^{n_{\rm b}-1} N_k, \tag{53}$$

where $n_{\rm b}$ is the total number of batches. The root mean squares of eccentricities and inclinations of planetesimals are given by

$$\langle e^{*2} \rangle^{1/2} \equiv \sqrt{\frac{\sum_{j=0}^{n_{\rm b}-1} N_j e_j^{*2}}{N_{\rm c}(m_0)}} \quad \text{and} \quad \langle i^{*2} \rangle^{1/2} \equiv \sqrt{\frac{\sum_{j=0}^{n_{\rm b}-1} N_j i_j^{*2}}{N_{\rm c}(m_0)}}, \tag{54}$$

respectively. The root mean square of masses of all planetesimals is defined in the same way.

(a) Case with nebular gas. Kokubo and Ida (1996) showed that the mass distribution of planetesimals is described by a single power law as $n_{\rm s}(m)\,dm \propto m^{-2.5}\,dm$ just after the runaway growth starts. Kokubo and Ida (2000) began their calculation of the accumulation process by use of the power-law initial mass distribution. The minimum mass of the distribution, m_0, is taken as 2×10^{23} g and the mass of the largest body is $20m_0$. The total mass of planetesimals is set to be $6507m_0$. The initial dispersions of the eccentricity and the inclination of planetesimals are assumed to be

$$e_0^* = 2i_0^* = 0.002. \tag{55}$$

We show snapshots of the cumulative number of the mass distribution at $t = 1 \times 10^5$, 2×10^5, and 4×10^5 years in Fig. 4. The initial mass distribution ($t = 0$ year) is shown in the first snapshot by the dashed curve. In Fig. 5, the corresponding

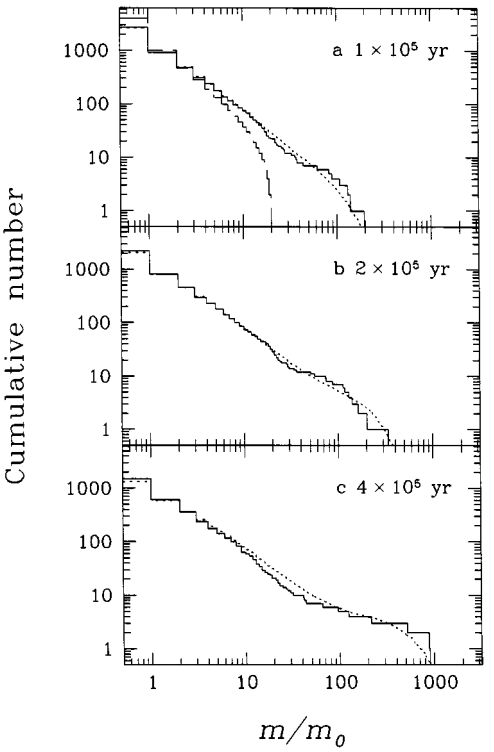

FIG. 4. Comparison between the cumulative numbers obtained from the statistical method (dotted curve) and the N-body simulation (solid curve) at $t =$ (a) 1×10^5, (b) 2×10^5, and (c) 4×10^5 years. Initial mass distribution is also shown by the dashed curve in (a).

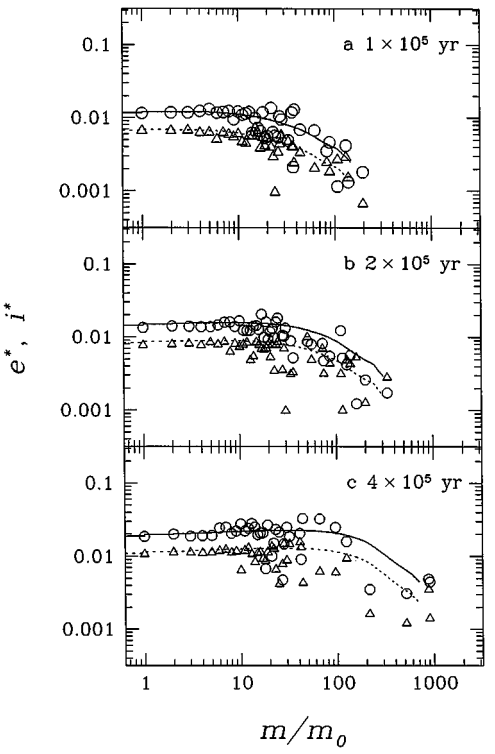

FIG. 5. Comparison between e^* and i^* calculated by the statistical method (solid and dashed curves) and the N-body simulation (circles and triangles) at $t =$ (a) 1×10^5, (b) 2×10^5, and (c) 4×10^5 years.

snapshots of the dispersions of eccentricities and inclinations are shown. At $t = 1 \times 10^5$ years, bodies with masses larger than $100m_0$ begin to form. Their dispersions of eccentricities and inclinations are suppressed by dynamical friction from small bodies. Eccentricity and inclination dispersions of small bodies with masses between m_0 and $10m_0$ are nearly independent of mass. The mass range of planetesimals with constant e^* and i^* spreads with time, and the eccentricity and the inclination increase monotonically with the growth of the bodies at the high-mass end. At $t = 4 \times 10^5$ years, planetesimals with masses smaller than $200m_0$ have almost the same e^* and i^*, which are 1.6 times larger than those at $t = 1 \times 10^5$ years.

In Fig. 4, we see that in the mass range of m_0 to $10m_0$ at any time the cumulative number calculated from the N-body simulation and the statistical method coincide with each other almost completely. For the relatively large bodies, there is a minor difference in the cumulative numbers. The cumulative number of planetesimals with $30m_0$ given by the N-body simulation is 1.7 times smaller than that found by the statistical method. The difference is about two times as large as a standard deviation and may be a systematic error. However, generally both results agree well with each other. As may be seen in Fig. 5, e^* and i^* of small bodies in the N-body simulation agree with those in the statistical method. For large bodies, it is difficult to compare them because of the statistical fluctuation in the N-body simulation. The values of i^* of the N-body simulation seem to be consistently lower for large bodies. However, the trends of the two results resemble each other.

Figure 6a shows the time evolution of the mass of the largest body, $M_{\max}$, and the root mean square of the mass of all the planetesimals, $\langle m^2 \rangle^{1/2}$. Initially the mass of the largest body is $20m_0$ and becomes about $1000m_0$ at $t = 5 \times 10^5$ years. In Fig. 6a, the ensemble mean $M_{\max}$, and the curves of $M_{\max} + \sigma_M$ and $M_{\max} - \sigma_M$ are shown, where σ_M is the standard deviation of the mass of the largest body obtained from the results of 100 runs. Despite the discontinuous evolution of $M_{\max}$ in the N-body simulation, it almost always remains within the region bounded by $M_{\max} + \sigma_M$ and $M_{\max} - \sigma_M$. Figure 6b shows the time evolution of the root mean squares of eccentricities, $\langle e^{*2} \rangle^{1/2}$ and inclinations, $\langle i^{*2} \rangle^{1/2}$ for all planetesimals. They increase monotonically with time. As in Fig. 6a, the ensemble means $\overline{\langle e^{*2} \rangle^{1/2}}$ and $\overline{\langle i^{*2} \rangle^{1/2}}$ and $\overline{\langle e^{*2} \rangle^{1/2}} \pm \sigma_e$ and $\overline{\langle i^{*2} \rangle^{1/2}} \pm \sigma_i$ are shown. The root mean square values obtained by the N-body simulation almost fall within the regions bounded by $\overline{\langle e^{*2} \rangle^{1/2}} \pm \sigma_e$ and $\overline{\langle i^{*2} \rangle^{1/2}} \pm \sigma_i$. Thus, we can say that the statistical method succeeds in reproducing the results of the N-body simulation very well.

The orbital separation of the runaway bodies δa_i is the only free parameter used in our statistical method and it is set at 10 Hill radii in the above calculation. We perform two additional calculations with different orbital separations, $\delta a_i = 5$ and 15 Hill radii, to see the dependence on the orbital separation. Figure 7 shows the ensemble means of the masses of the largest bodies obtained by the statistical simulations with various orbital separations, as well as that of the N-body simulation. In the case of $\delta a_i = 15$ Hill radius, the runaway body grows too

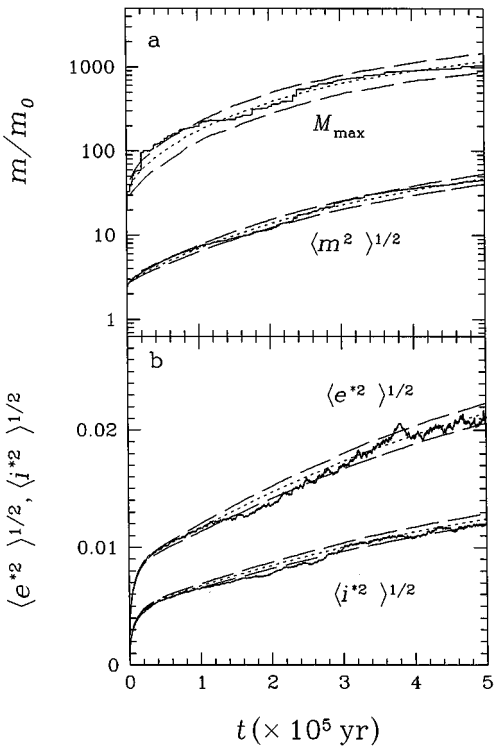

FIG. 6. Time evolution of the mass of the largest body, $M_{\max}$, and the root mean square of mass, $\langle m^2 \rangle^{1/2}$ (a). The dotted and dashed curves correspond to $M_{\max}$ and $M_{\max} \pm \sigma_M$ obtained by the statistical method, respectively, where $M_{\max}$ and σ_M are the ensemble mean and its standard deviation obtained from the statistical simulations. The solid curves are of the N-body simulation. Time evolution of the root mean squares of eccentricities and inclinations of planetesimals is shown in (b).

fast because a large value of δa_i allows a pair of large bodies with a small separation to collide. In the case of 5 Hill radius, on the other hand, the growth of the runaway bodies is slow compared with that in the N-body simulation. Hence, $\delta a_i = 10$

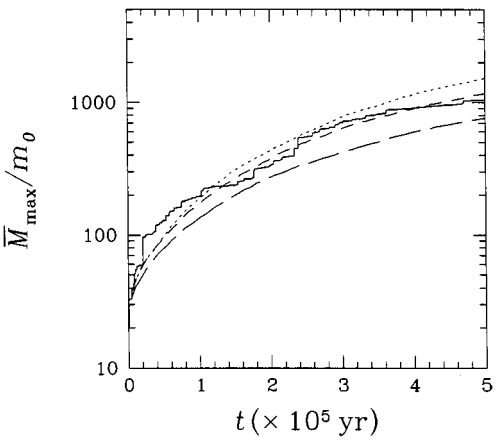

FIG. 7. Evolution of the expectation value of the mass of the largest body obtained by the statistical method with three different orbital separations. Dotted line, short dashed line, and long dashed line are the results for $\delta a_i = 15, 10$, and 5 Hill radii, respectively. The result of the N-body simulation (Kokubo and Ida 2000) is also shown by the solid curve.

Hill radii reproduces the result of the N-body simulation best. This is accordance with the results in Kokubo and Ida (1998) where the orbital separation of the runaway bodies is given as 10 Hill radii.

(b) Case without nebular gas. We also make a comparison with the N-body simulation for the case without nebular gas (see Table I). The initial mass, m_0, and the total number of planetesimals are chosen to be 3×10^{23} g and 4000, respectively. The initial dispersions of eccentricities and inclinations are given by $e_0^* = 2i_0^* = 0.0018$.

The time evolution of the mass of the largest body, $M_{\max}$, and the root mean square masses, $\langle m^2 \rangle^{1/2}$, are shown in Fig. 8a. The root mean squares of eccentricities, $\langle e^{*2} \rangle^{1/2}$, and inclinations, $\langle i^{*2} \rangle^{1/2}$, are shown in Fig. 8b. In these figures, $M_{\max}$ and $M_{\max} \pm \sigma_M$, obtained by the statistical method, are shown in a way similar to those of Fig. 6. For the mass of the largest body and the root mean square masses, the statistical method gives the same evolution curve as that of the N-body simulation. While the N-body simulation gives a root mean square of inclinations slightly smaller than $\overline{\langle i^{*2} \rangle^{1/2}} - \sigma_i$, the root mean square of eccentricities obtained by the N-body simulation is bounded by $\overline{\langle e^{*2} \rangle^{1/2}} \pm \sigma_e$. However, the difference is quite small, confined within a factor of 1.07. Consequently, regardless of whether we consider planetary accumulation with or without nebular gas, the statistical method can describe the accumulation process of planetesimals very accurately.

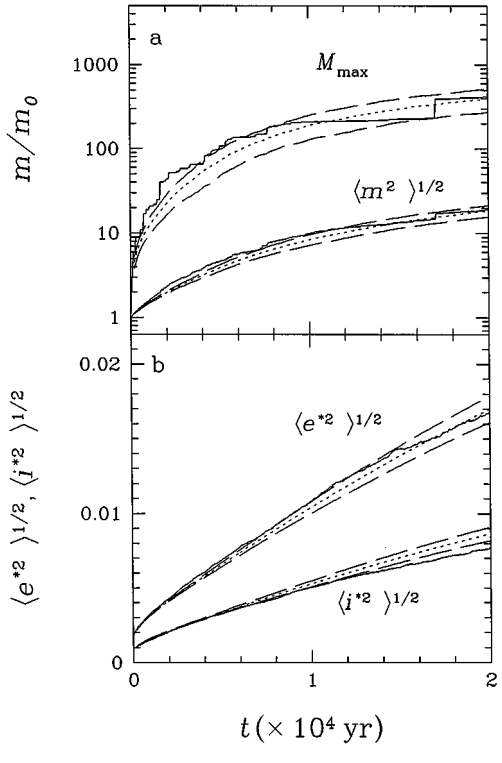

FIG. 8. The same as described in the legend to Fig. 6, but for the case without nebular gas.

4.2. Relationship to Previous Statistical Simulation

A number of calculations of planetary accumulation have been carried out by use of the statistical method (e.g., Greenberg *et al.* 1978; Nakagawa *et al.* 1983; Ohtsuki *et al.* 1988; Barge and Pellat 1991, 1993; Spaute *et al.* 1991; Wetherill and Stewart 1989, 1993; Weidenschilling *et al.* 1997; Kenyon and Luu 1998, 1999). An early major contribution was made by Stewart and Kaula (1980) in introducing the importance of dynamical friction, now recognized as the process that is principally responsible for runaway growth. This was later illustrated by Stewart and Wetherill (1988), Spaute *et al.* (1991), and Wetherill and Stewart (1989, 1993). Following the introduction of dynamical friction into consideration of this problem, the short ($\sim 10^5$ years) time scale for the formation of $\sim 10^{26}$ g bodies at 1 AU became generally accepted. In the absence of dynamical friction, $\sim 10^6$ years is required for the largest body to grow to 10^{24} g, the size of Ceres, whereas when dynamical friction is included, bodies larger than $\sim 10^{26}$ g (Moon to Mercury size) can be formed within $\sim 10^5$ years.

The approach taken by many of these authors differs from the present work in that the velocity evolution is based on the Fokker–Planck equation and Boltzmann equation, following the work of Hornung *et al.* (1985). Wetherill and Stewart (1993, henceforth called WS93) included the effect of collisional fragmentation, which was also considered by Greenberg *et al.* (1978), Barge and Pellat (1993), and Kenyon and Luu (1999). In the absence of fragmentation, runaway growth tends to be attenuated since the smaller bodies are accelerated to high velocities. More realistically, when fragmentation is included, this effect will be truncated by collisional fragmentation, producing small fragments, the velocity of which is reduced by gas drag. A unique contribution is that of Weidenschilling *et al.* (1997), which is still the only statistical calculation that also includes changes in the semimajor axis of the growing planetary bodies. That work unifies the processes of accumulation of an initial population of very small bodies with final oligarchic growth. Although quantitatively these results differ somewhat from those of other investigations, they provide further support for this model of planetary accumulation.

In earlier work on the "planetesimal problem," the goal of the investigation was first to analyze the validity of the concept of runaway growth, and to later establish that it was a robust process, one that can be expected to prevail over the earlier concept of "orderly growth." This goal was successfully accomplished. It was found that runaway growth was not strongly dependent on the details of the model. This conclusion has been confirmed by other workers and can be considered to be well established. In this context, the authors did not consider it a matter of immediate interest to know if 10,000 years or 20,000 years were required to initiate the bimodal mass distribution characteristic of runaway growth. Both of these values of elapsed time were probably shorter than the timescale of the addition of material to the protoplanetary disk.

The present authors have a different goal, which is to improve this situation by providing a more rigorous and user friendly generic program that can supplant those earlier efforts, and thereby provide a more sound basis for further progress, an opportunity that was made possible by many contributions during recent years (Greenzweig and Lissauer 1992, Ohtsuki 1999, SI00). As an example of use of this opportunity, a comparison of the "nominal model" of WS93 for the case of planetary growth without collisional fragmentation will be given here. In this comparison, we set the orbital separation of the runaway bodies to be the same as WS93, i.e., $\delta a_i = 2\sqrt{3}h_{m_i m_{\text{runaway}}}a + 2ae_i$, where e_i is the eccentricity of runaway body i. We also use the same initial mass, $m_0(4.8 \times 10^{18}$ g), and other parameters.

The results of the earlier nominal model calculation were given in Figs. 1 and 2 of WS93, including the effects of collisional fragmentation. Because the present work does not include collisional fragmentation, this calculation was replaced using the same program as WS93, but with omission of the fragmentation algorithm. This comparison is shown in Fig. 9. The WS93 calculations are represented in the upper pair of diagrams, and those of the present work in the lower pair.

On the whole, the results of the two calculations are similar in appearance. The most striking difference occurs early in the calculation at 10,000 years. In the present work, the largest body at this time has a mass of about 2.6×10^{22} g, whereas at this same time the largest body in WS93 has a mass of 7.6×10^{24} g, about 290 times larger. This difference is also reflected in the values of horizontal velocity (proportional to eccentricity). The latter difference is primarily caused by the stronger perturbations associated with larger bodies. At later times, the results are more similar, but the final single largest body in WS93 has a mass about three times that using the present program. Another easily noted difference is the more extended "flat region" in the cumulative number distributions of WS93, regions in which bodies are completely absent.

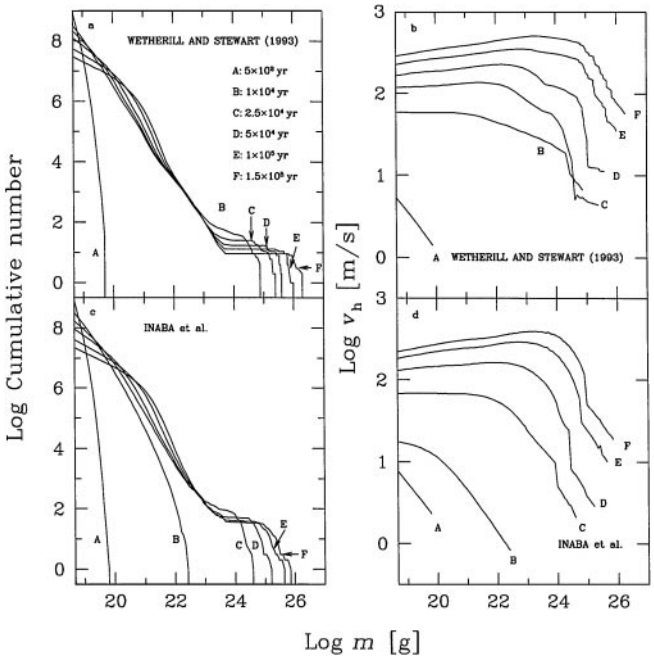

FIG. 9. Snapshots of the cumulative number and the horizontal velocities. The numerical results of Wetherill and Stewart (1993) are shown in (a) and (b), while those of our code in (c) and (d).

The major differences between the present program and that of WS93 are:

(1) The changes in velocity caused by collisions are treated in different ways in the two calculations. In WS93, they were based on use of the Boltzmann equation for inelastic collisions as described in Stewart and Wetherill (1988). They considered the change in velocities of colliding planetesimals, assuming that the restitution coefficients are 0. Following this method, the velocities of colliding bodies are damped by inelastic collision, instead of that of the merger of colliding bodies. In the present work they are obtained from Eqs. (31) and (32), where the velocity changes resulting from the merger of colliding bodies were calculated for perfectly inelastic accumulation into a sphere.

(2) The work of SI00 demonstrated that the effects of long-range perturbations were greater than was thought earlier, particularly between bodies of low relative velocities. Long-range perturbations were included in WS93 only by the addition of an term of +0.55 in the ln Λ term of Eq. (c2) in the velocity change algorithms, as proposed by Weidenschilling (1989). Insofar as it is valid, this term should have been introduced only for the changes in eccentricity for viscous stirring.

The effects of taking these differences into consideration are illustrated in Fig. 10. In this calculation, the present program was modified to calculate velocity changes caused by collisional damping in the same way as in WS93. In addition, long-range perturbations were omitted in the calculation using the present program. When these changes were made, comparison of the WS93 results in the upper part of Fig. 9 with this modified present program in the lower pair of Fig. 10 shows that omission of these two aspects of the present program reduces considerably the differences discussed earlier.

This comparison has been carried further by reference to the upper part of Fig. 10. Here some changes have been made in the WS93 program:

(1) The time step was reduced from 0.5 to 0.1 years in order to reduce errors from using a time step that was too long. This is made possible because the work station used now is 175 times faster than those used for the calculations in WS93. As a result, a calculation can be finished in a few hours that required months in 1993.

(2) Because all of the long-range perturbations were removed from the present model, for consistency, the additive terms of +0.55, introduced as an approximate way of introducing long-range perturbations, should be removed from the WS93 calculation as well. This was done for all the velocity change algorithms of WS93, with the exception of that for viscous stirring. For

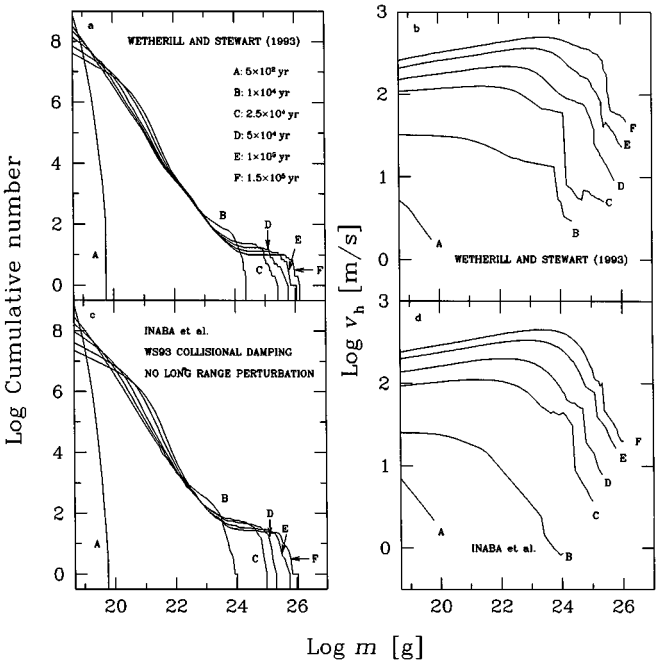

FIG. 10. The same as described in the legend to Fig. 9, but for the case that long-range perturbation is not included and velocity change due to collisions derived by Stewart and Wetherill (1988) are used.

viscous stirring the value of this term was reduced from 0.55 to 0.05. This was done because complete removal of the additive term resulted in some degree of instability in the velocity algorithm. Comparison of this calculation and one with the additive term equal to 0.10 instead of 0.05 showed very little difference.

(3) Comparison of the derivation of the growth algorithm used in WS93 and that in the present work showed that the "particle in a box" algorithm used in WS93, based on Safronov (1969) resulted in it being a factor of 1.3 larger than that used in the present work, based on Eq. (2) (Nakazawa *et al.* (1989), Ohtsuki (1999)). This algorithm was changed to match that of the present program.

(4) As discussed by Safronov (1969, Eq. (7.86)), the large runaway bodies become less effective perturbers of the smaller bodies because of the approximate conservation of the Jacobi parameter, and "control" is transfered to the second larger body with which they interact. This effect was included in WS93 (Section IIC), but not in the present investigation. Reasons were given in WS93 (p. 196) for thinking this effect was of minor importance, and these same reasons are valid in the present calculation. Some further support for this calculation is provided in Figs. 4 and 5 in which it is seen that the present program is in good agreement with numerical integration, for which the circumstances considered by Safronov are automatically included. For purposes of comparison, this effect is not included in the calculation of Fig. 10.

(5) By private communications in 1996 and 1997, G. Stewart provided information regarding errors in the coefficient in the velocity change algorithms equations given in Appendix C of WS93. These are now described in SI00. These changes are included in the calculation of Fig. 10. They were found to cause very little difference in the results.

The consequences of these additional changes may be seen by comparison of the upper diagrams of Fig. 9 with those of Fig. 10. Although noticeable, they are not dramatic. An easily noticed difference between the present calculation and that of the "modified" WS93 calculation in Fig. 10 is that between the velocity distribution at 10,000 years. In this method WS93 calculation, at 8800 years the largest body reached the same mass of that of the present calculation at 10,000 years. If the velocity evolution had been plotted at 8800 years instead of 10,000 years in the upper figures of Fig. 10, this would also appear very similar to that of curve B in the figure below it, representing the results of the present investigations.

It may be noticed that WS93 also contains a calculation in which fragmentation was not included (WS93, Fig. 12). This was not used in the present comparison, because we have found that it made use of an earlier version of the growth algorithm that was somewhat different from that used in the nominal model. If this calculation had been used for comparison, the result would have looked more favorable. Because this would cause the comparison to appear to be better than is justified, we used the standard model, described in detail WS93 (WS93, Fig. 1), but calculated without fragmentation. At the time this earlier work was carried out, differences of this magnitude were not thought to be of interest.

It should not be concluded from this moderately satisfactory outcome of this discussion that these two programs are nearly equivalent. The approximate agreement between the results at 10,000 years was achieved only by removing the effects of real phenomena from the present calculations. Furthermore, SI00 reports further changes that should be made in order to develop a state-of-the-art accumulation program based on transport theory. However, these modifications still would not provide an independent way of including long-range perturbations or of including accelerations in the low-velocity regime. We conclude that the WS93 program made a timely contribution at an earlier stage of development of the theory of planetesimal accumulation, and we look forward to the time at which the present work can be described in the same way, in this case not because of differences in the basic equations, but as a consequence of the idealization of the real processes of planetary formation that are still necessary at the present time.

This program has been used in Wetherill and Inaba (2000) to investigate the consequences of assuming that the initial planetesimals were added on a long timescale of $\sim 10^5$ years, rather than forming instantaneously, as previously assumed. The reason of interest is that one might wonder how this initial distribution arose in the first place, in as much as it is found to be unstable with respect to rapid growth. The investigation discussed shows that quite similar runaway growth occurs on a $\sim 10^5$ year timescale, even though the initial bodies are formed

gradually on a similar timescale. However, it was also found that initial mass bodies that were added in the later stage of growth did not follow the earlier chain of accumulation. Instead, their relative velocities quickly became sufficiently high to fragment them. These fragments then either were directly accumulated by the runaway bodies or drifted toward the Sun by gas drag.

5. CONCLUDING COMMENTS

We have constructed a statistical code that makes use of the latest results of basic processes such as the collision rate between planetesimals and the evolution of kinetic properties of planetesimals. The accuracy of this code has been tested by comparison with results obtained by N-body simulation (Kokubo and Ida 1998, 2000). Comparisons have been made with and without nebular gas. It is found that the statistical code can reproduce the results of the N-body simulation with high accuracy. The time evolution of the mass of the largest bodies given by both simulations agrees well with one another. Thus, the statistical method developed in the present study can describe the accumulation process of planetesimals more precisely than the previous statistical programs.

While of basic importance to this investigation, at the present time, numerical N-body simulations cannot include the effects of the very large number of bodies in the complete mass range of bodies that occur in the process of planetary formation. It is also difficult for N-body studies to include the wide range of parameter space of the physical parameters that may be expected to occur in other planetary systems. Furthermore, complete treatment of many difficult problems must address processes that cannot be treated in the rigorous way that we have been able to do for this idealized model. These include processes such as collisional fragmentation of the bodies and inclusion of the radial dimension of planetary formation. The present program can serve to provide a firm basis for addressing these more difficult problems, the solution of which will be necessary in order to achieve a more clear understanding of the formation of planetary systems.

APPENDIX

In this Appendix, we will derive the expression of $\langle P_{\rm VS}\rangle$ for the gravitational stirring between runaway bodies. Generally, the stirring rate $\langle P_{\rm VS}\rangle$ is defined as

$$\langle P_{\rm VS}\rangle \equiv \int \Delta\tilde{e}^2 \frac{3}{2}|\tilde{b}|\, d\tilde{b}\frac{d\tau\, d\omega}{(2\pi)^2} f(\tilde{b},\tilde{e},\tilde{i})\, d\tilde{e}\, d\tilde{i}, \tag{56}$$

where

$$\tilde{b} \equiv \frac{a_2 - a_1}{a h_{12}}, \tag{57}$$

and a_1 and a_2 are the semimajor axes of planetesimals and h_{12} is given by Eq. (3) and $\Delta\tilde{e}^2$ is the change of the square of the reduced relative eccentricity (Eq. (6)) during an encounter. The distribution function of planetesimals $f(\tilde{b},\tilde{e},\tilde{i})$ is expressed as

$$f(\tilde{b},\tilde{e},\tilde{i}) = f_{\rm S}(\tilde{b}) f_{\rm R}(\tilde{e},\tilde{i}). \tag{58}$$

When $f_{\rm S}(\tilde{b}) = 1$, Eq. (56) agree with that given by Ohtsuki (1999). In the case where runaway bodies orbit around the central star keeping their mutual distance $\Delta\tilde{b}$, $f_{\rm S}(\tilde{b})$ is given by

$$f_{\rm S}(\tilde{b}) = \Delta\tilde{b}\sum_{n=1}^{\infty}(\delta(\tilde{b} - n\Delta\tilde{b}) + \delta(\tilde{b} + n\Delta\tilde{b})), \tag{59}$$

where $\delta(x)$ is the delta function. Hasegawa and Nakazawa (1990) evaluated the change of the square of the reduced eccentricity averaged over the phase space as

$$\langle \Delta\tilde{e}^2\rangle \equiv \int \Delta\tilde{e}^2 \frac{d\tau\, d\omega}{(2\pi)^2} = \frac{45}{\tilde{b}^4}. \tag{60}$$

From Eqs. (56), (59), and (60), we have

$$\langle P_{\rm VS}\rangle = \frac{160}{\Delta\tilde{b}^2}. \tag{61}$$

Remembering $\Delta\tilde{b} = 10$ according to Eq. (43), we find

$$\langle P_{\rm VS}\rangle = 1.6. \tag{62}$$

ACKNOWLEDGMENTS

We express our gratitude to S. Ida for helpful discussion. We also thank H. Emori and S. J. Kortenkamp for continuous encouragement. This work has been supported by a Grant-in-Aid for General Scientific Research (B) (No. 09440089) and by NASA Grants NAG5-6873, NAG5-4285, and NAG5-6977. S. Inaba is grateful for financial support from the Japan Society for Promotion of Science (JSPS Postdoctoral Fellowships for Research Abroad, 1999–2001). The computation has been performed on Cray C916 at the Computer Center of Tokyo Institute of Technology and a Alpha PC at the Carnegie Institution of Washington.

REFERENCES

Adachi, I., C. Hayashi, and K. Nakazawa 1976. The gas drag on the elliptic motion of a solid body in the primordial solar nebula. *Prog. Theor. Phys.* **56**, 1756–1771.

Barge, P., and R. Pellat 1991. Mass spectrum and velocity dispersions during planetesimal accumulation. I. Accretion. *Icarus* **93**, 270–287.

Barge, P., and R. Pellat 1993. Mass spectrum and velocity dispersions during planetesimal accumulation. II. Fragmentation. *Icarus* **104**, 79–96.

Dones, L., and S. Tremaine 1993. On the origin of planetary spins. *Icarus* **103**, 67–92.

Greenberg, R., J. Wacker, C. R. Chapman, and W. K. Hartmann 1978. Planetesimals to planets: Numerical simulation of collisional evolution. *Icarus* **35**, 1–26.

Greenzweig, Y., and J. J. Lissauer 1990. Accretion rates of protoplanets. *Icarus* **87**, 40–77.

Greenzweig, Y., and J. J. Lissauer 1992. Accretion rates of protoplanets II. Gaussian distributions of planetesimal velocities. *Icarus* **100**, 440–463.

Hasegawa, M., and K. Nakazawa 1990. Distant encounter between Keplerian particles. *Astron. Astrophys.* **227**, 619–627.

Hornung, P., R. Pellat, and P. Barge 1985. Thermal velocity equilibrium in the protoplanetary cloud. *Icarus* **64**, 295–307.

Ida, S. 1990. Stirring and dynamical friction of planetesimals in the solar gravitational field. *Icarus* **88**, 129–145.

Ida, S., and J. Makino 1992a. *N*-body simulation of gravitational interaction between planetesimals and a protoplanet. I. Velocity distribution of planetesimals. *Icarus* **96**, 107–120.

Ida, S., and J. Makino 1992b. *N*-body simulation of gravitational interaction between planetesimals and a protoplanet. II. Dynamical friction. *Icarus* **98**, 28–37.

Ida, S., and K. Nakazawa 1989. Collisional probability of planetesimals revolving in the solar gravitational field. III. *Astron. Astrophys.* **224**, 303–315.

Inaba, S., H. Tanaka, K. Ohtsuki, and K. Nakazawa 1999. High-accuracy statistical simulation of planetary accretion: I. Test of the accuracy by comparison with the solution to the stochastic coagulation equation. *Earth Planets Space* **51**, 205–217.

Kary, D. M., J. J. Lissauer, and Y. Greenzweig 1993. Nebular gas drag and planetary accretion. *Icarus* **106**, 288–307.

Kenyon, S. J., and J. X. Luu 1998. Accretion in the early Kuiper belt. I. Coagulation and velocity evolution. *Astron. J.* **115**, 2136–2160.

Kenyon, S. J., and J. X. Luu 1999. Accretion in the early Kuiper belt. II. Fragmentation. *Astron. J.* **118**, 1101–1119.

Kokubo, E., and S. Ida 1996. On runaway growth of planetesimals. *Icarus* **123**, 180–191.

Kokubo, E., and S. Ida 1998. Oligarchic growth of protoplanets. *Icarus* **131**, 171–178.

Kokubo, E., and S. Ida 2000. Formation of protoplanets from planetesimals in the solar nebula. *Icarus* **143**, 15–27.

Marcus, A. H. 1968. Stochastic coalescence. *Technometrics* **10**, 133–143.

Nakagawa, Y., C. Hayashi, and K. Nakazawa 1983. Accumulation of planetesimals in the solar nebula. *Icarus* **54**, 361–376.

Nakazawa, K., S. Ida, and Y. Nakagawa 1989. Collisional probability of planetesimals revolving in the solar gravitational field I. Basic formulation. *Astron. Astrophys.* **220**, 293–300.

Ohtsuki, K. 1992. Evolution of random velocities of planetesimals in the course of accretion. *Icarus* **98**, 20–27.

Ohtsuki, K. 1999. Evolution of particle velocity dispersion in a circumplanetary disk due to inelastic collisions and gravitational interactions. *Icarus* **137**, 152–177.

Ohtsuki, K., Y. Nakagawa, and K. Nakazawa 1988. Growth of the earth in nebula gas. *Icarus* **75**, 552–565.

Ohtsuki, K., S. Ida, Y. Nakagawa, and K. Nakazawa 1993. Planetary accretion in the solar gravitational field. In *Protostars and Planets III* (E. H. Levy and J. I. Lunine, Eds.), pp. 1061–1088. Univ. of Arizona Press, Tucson.

Safronov, V. S. 1969. *Evolution of the Protoplanetary Cloud and Formation of the Earth and Planets. Nauka, Moscow.* [Transl. 1972 NASA TT 6-77.]

Spaute, D., S. J. Weidenschilling, D. R. Davis, and F. Marzari 1991. Accretional evolution of a planetesimal swarm: 1. A new simulation. *Icarus* **92**, 147–164.

Stewart, G. R., and S. Ida 2000. Velocity evolution of planetesimals: Unified analytical formulae and comparison with *N*-body simulations. *Icarus* **143**, 28–44.

Stewart, G. R., and W. M. Kaula 1980. Gravitational kinetic theory for planetesimals. *Icarus* **44**, 154–171.

Stewart, G. R., and G. W. Wetherill 1988. Evolution of planetesimal velocities. *Icarus* **74**, 542–553.

Tanaka, H., and K. Nakazawa 1993. Stochastic coagulation equation and validity of the statistical coagulation equation. *J. Geomag. Geoelectr.* **45**, 361–381.

Weidenschilling, S. J. 1989. Stirring of a planetesimal swarm: The role of distant encounters. *Icarus* **80**, 179–188.

Weidenschilling, S. J., D. Spaute, D. R. Davis, F. Marzari, and K. Ohtsuki 1997. Accretional evolution of a planetesimal swarm 2. The terrestrial zone. *Icarus* **128**, 429–455.

Wetherill, G. W. 1990. Comparison of analytical and physical modeling of planetesimal accumulation. *Icarus* **88**, 336–354.

Wetherill, G. W., and L. P. Cox 1985. The range of validity of the two-body approximation in models of terrestrial planet accumulation. II. Gravitational cross sections and runaway accretion. *Icarus* **63**, 290–303.

Wetherill, G. W., and S. Inaba 2000. Planetary accumulation with a continuous supply of planetesimals. *Space Sci. Rev.* **92**, 311–320.

Wetherill, G. W., and G. R. Stewart 1989. Accumulation of a swarm of small planetesimals. *Icarus* **77**, 330–357.

Wetherill, G. W., and G. R. Stewart 1993. Formation of planetary embryos: Effects of fragmentation, low relative velocity, and independent variation of eccentricity and inclination. *Icarus* **106**, 190–209.